

Wrong-Helicity Electrons in Radiative Muon Decay

V. S. Schulz and L. M. Sehgal

*Institute of Theoretical Physics, RWTH Aachen
D-52056 Aachen, Germany*

Abstract

We have studied in detail the spectrum of the decay $\mu^- \rightarrow e^- \bar{\nu}_e \nu_\mu \gamma$ as a function of the electron helicity, and verify the prediction [1] that a significant fraction of the electrons in this decay is right-handed. These “wrong-helicity” electrons persist in the limit $\lambda = m_e/m_\mu \rightarrow 0$, and are connected with helicity-flip bremsstrahlung in QED. The longitudinal polarization of the electron is calculated as a function of the photon and electron energy, and deviates systematically from the naive V-A prediction $P_L = -1$. The right-handed component is concentrated in the collinear region $\theta \lesssim m_e/E_e$. In the limit $\lambda \rightarrow 0$, we reproduce the results obtained in [1] using the helicity-flip splitting function introduced by Falk and Sehgal.

1 Introduction

In a recent Letter [1] it was pointed out that as a consequence of helicity-flip bremsstrahlung, electrons in the radiative decay $\mu^- \rightarrow e^- \bar{\nu}_e \nu_\mu \gamma$ are not purely left-handed, even in the limit $m_e \rightarrow 0$. The decay width into right-handed electrons was shown to be $\Gamma_R = \frac{\alpha}{4\pi} \Gamma_0$, where $\Gamma_0 \equiv G_F^2 m_\mu^5 / (192\pi^3)$. The energy spectrum of these wrong-helicity electrons was calculated, as also that of the photons accompanying them. These results were obtained using the helicity-flip splitting function $D_{\text{hf}}(z) = \frac{\alpha}{2\pi} z$ introduced by Falk and Sehgal [2].

The appearance of right-handed electrons in μ -decay is, at first sight, surprising since it goes against the conventional wisdom based on the V-A structure of weak interaction and the common assumption of helicity-conservation in massless QED. However persistence of helicity-flip bremsstrahlung in the $m_e \rightarrow 0$ limit has been established in several calculations of radiative processes [3, 4, 5, 6, 7], going back to the seminal paper of Lee and Nauenberg [8]. In all cases, the origin of the effect is the characteristic behaviour of helicity-flip bremsstrahlung at small angles

$$d\sigma_{\text{hf}} \approx \left(\frac{m_e}{E_e}\right)^2 \frac{d\theta^2}{\left[\theta^2 + \left(\frac{m_e}{E_e}\right)^2\right]^2}, \quad (1)$$

leading to a non-zero integrated rate that survives the limit $m_e \rightarrow 0$.

In the present paper, we derive the helicity-dependent spectrum of the decay $\mu^- \rightarrow e^- \bar{\nu}_e \nu_\mu \gamma$ from first principles, without neglecting the electron mass. We obtain the longitudinal polarization P_L of the electron as a function of the electron energy, photon energy and the angle between the electron and photon. We then consider the limit $m_e \rightarrow 0$ to demonstrate that the deviation from $P_L = -1$ is present even in the chiral limit of QED. The results are compared with those obtained in the equivalent particle approach based on the helicity-flip fragmentation function, thus providing a confirmation of the statements in Ref.[1].

2 Matrix Element and Phase Space for $\mu^- \rightarrow e^- \bar{\nu}_e \nu_\mu \gamma$

The matrix element for the decay $\mu^- \rightarrow e^- \bar{\nu}_e \nu_\mu \gamma$ may be obtained from the Feynman diagrams shown in Fig.(1). Adopting the notation of Ref.[9, 10], we obtain the square of the matrix element, summed over the photon polarization, taking the muon to be unpolarized. The spectrum is derived in terms of the invariants

$$x := \frac{2p_\mu \cdot p_e}{m_\mu^2}, \quad y := \frac{2p_\mu \cdot k}{m_\mu^2}, \quad z := \frac{2p_e \cdot k}{m_\mu^2} \quad (2)$$

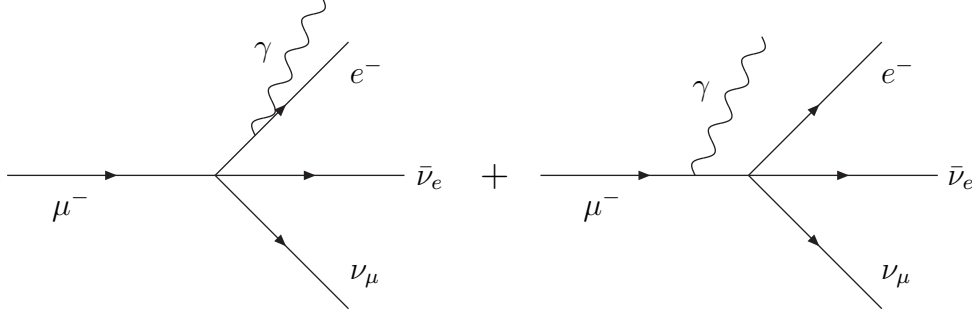


Figure 1: Feynman diagrams

and the mass ratio $\lambda := m_e/m_\mu$. In the rest frame of the muon,

$$x = \frac{2E_e}{m_\mu}, \quad y = \frac{2E_\gamma}{m_\mu}, \quad z = \frac{y}{2} [x - \cos(\theta) \sqrt{x^2 - 4\lambda^2}], \quad (3)$$

E_e, E_γ being the energies of the electron, photon and $\cos(\theta)$ the angle between them. The boundary of phase space is determined by the condition $-1 \leq \cos(\theta) \leq 1$, and $0 \leq Q^2 \leq (1 - \lambda)^2 m_\mu^2$, Q^2 being the “missing mass” of the neutrino pair. This leads to the condition

$$0 \leq y \leq y_m(x), \quad 2\lambda \leq x \leq 1 + \lambda^2, \quad (4)$$

where

$$y_m(x) = 2 \frac{1 + \lambda^2 - x}{2 - x + \sqrt{x^2 - 4\lambda^2}}. \quad (5)$$

Equivalently, the limits of phase space may be expressed as

$$2\lambda \leq x \leq x_m(y), \quad 0 \leq y \leq 1 - \lambda, \quad (6)$$

where

$$x_m(y) = \frac{\lambda^2 + (1 - y)^2}{1 - y}. \quad (7)$$

The differential decay width for $\mu^- \rightarrow e^- \bar{\nu}_e \nu_\mu \gamma$ in the variables x, y and $\cos(\theta)$ is then given by

$$\left(\frac{d\Gamma}{dx dy d\cos(\theta)} \right)_{\text{R,L}} = (-1) \Gamma_0 \frac{\alpha}{2\pi} \sqrt{x^2 - 4\lambda^2} \frac{1}{y} \frac{1}{z^2} \frac{1}{2} (g_0 \pm g_1) \quad (8)$$

where R and L denote right-handed and left-handed electrons, corresponding to the polarization vectors

$$(s_e)_{\text{R}} = \left(\frac{|\mathbf{p}_e|}{m_e}, \frac{E_e}{m_e} \hat{\mathbf{p}}_e \right) \quad (s_e)_{\text{L}} = \left(\frac{|\mathbf{p}_e|}{m_e}, -\frac{E_e}{m_e} \hat{\mathbf{p}}_e \right). \quad (9)$$

The functions g_0 and g_1 are given by

$$\begin{aligned} g_0 := & -2xy z^2 + 6xy z^3 - 6x y^2 z - 8x y^2 z^2 + 6x y^3 z + 6x z^2 + 8x z^3 - 6x^2 y z - 8x^2 y z^2 \\ & + 8x^2 y^2 z - 4x^2 z^2 + 4x^3 y z + 6y z^2 + 5y z^3 - 2y z^4 - 2y^2 z^2 + 2y^2 z^3 - 3y^3 z - 2y^3 z^2 \\ & + 2y^4 z - 6z^3 - 4z^4 \\ & + \lambda^2 (8xyz + 6xy z^2 + 2x y^2 z + 6x y^2 - 8x y^3 + 6x z^2 - 6x^2 y z - 4x^2 y^2 + 6y z^2 - 3y z^3 \\ & \quad - 6y^2 z - 2y^2 z^2 + 5y^3 z + 6y^3 - 4y^4 - 8z^2 - 6z^3) \\ & + \lambda^4 (6x y^2 - 6y^2 z - 8y^2 + 6y^3), \end{aligned} \quad (10)$$

$$\begin{aligned}
g_1 := & \left\{ 6x^3yz - 4x^4yz + 6x^2y^2z - 8x^3y^2z + 3xy^3z - 6x^2y^3z - 2xy^4z - 6x^2z^2 + 4x^3z^2 \right. \\
& - 6xy z^2 + 2x^2y z^2 + 8x^3y z^2 + 2xy^2z^2 + 8x^2y^2z^2 + 2xy^3z^2 + 6xz^3 - 8x^2z^3 \\
& - 5xy z^3 - 6x^2y z^3 - 2xy^2z^3 + 4xz^4 + 2xyz^4 \\
& + \lambda^2 (-6x^2y^2 + 4x^3y^2 - 6xy^3 + 8x^2y^3 - 6y^4 + 8xy^4 - 24xyz + 16x^2yz - 4y^2z^3 \\
& + 4y^5 + 2x^3yz + 22xy^2z - 6x^2y^2z + 4y^3z - 7xy^3z - 4y^4z + 24z^2 - 16xz^2 - 2x^2z^2 \\
& - 16yz^2 - 18xyz^2 - 2x^2yz^2 - 6y^2z^2 + 10xy^2z^2 + 4y^3z^2 + 16z^3 + 2xz^3 + xyz^3) \\
& + \lambda^4 (24y^2 - 16xy^2 - 2x^2y^2 - 16y^3 - 2xy^3 - 2y^4 - 8xyz + 16y^2z + 2xy^2z - 4y^3z \\
& + 8z^2 - 2y^2z^2) \\
& \left. + 8\lambda^6 y^2 \right\} \cdot \frac{1}{2\sqrt{x^2 - 4\lambda^2}}.
\end{aligned} \tag{11}$$

Adding the expressions for $d\Gamma_R$ and $d\Gamma_L$, we obtain the spectrum for unpolarized electrons, which depends on the function g_0 only [10]. The specific effects of electron helicity are contained in the function g_1 .

3 Unpolarized Spectra (summed over electron helicity)

Summing over the electron helicity, the differential decay rate of $\mu^- \rightarrow e^- \bar{\nu}_e \nu_\mu \gamma$ is

$$\left(\frac{d\Gamma}{dx dy d\cos(\theta)} \right)_{R+L} = (-1) \Gamma_0 \frac{\alpha}{2\pi} \sqrt{x^2 - 4\lambda^2} \frac{1}{y z^2} g_0. \tag{12}$$

From this we can derive the following spectra.

3.1 Dalitz plot in electron and photon energies

$$\begin{aligned}
\left(\frac{d\Gamma}{dx dy} \right)_{R+L} &= (-1) \Gamma_0 \frac{\alpha}{2\pi} \int_{-1}^{+1} d\cos(\theta) \sqrt{x^2 - 4\lambda^2} \frac{1}{y z^2} g_0(x, y, z; \lambda) \\
&= \Gamma_0 \frac{\alpha}{6\pi} \frac{1}{y} \left(\mathcal{A} \{ 12y(-6 + 3y + y^2) + x(-72 + 78y + 33y^2 - 6y^3) \right. \\
&\quad + 2x^2(24 + 12y - 5y^2 + 2y^3) \\
&\quad + \lambda^2 [96 - 72y + 4y^2 - 4y^3 + 9x(-8 - 2y + y^2)] \} \\
&\quad + 12\mathcal{L} \{ -4x^3 + x^2(6 - 8y) + 6\lambda^4 y - 6x(-1 + y)y + (3 - 2y)y^2 \\
&\quad \left. + \lambda^2 [6x^2 + (6 - 5y)y - 2x(4 + y)] \} \right),
\end{aligned} \tag{13}$$

where we have defined

$$\mathcal{A} := \sqrt{x^2 - 4\lambda^2}, \quad \mathcal{L} := \frac{1}{2} \log \left(\frac{x + \mathcal{A}}{x - \mathcal{A}} \right). \tag{14}$$

3.2 Photon Energy Spectrum

The photon energy spectrum $(d\Gamma/dy)_{R+L}$ is given explicitly in Eq.(A.1) of the Appendix. The leading term for small y (small photon energies) is

$$\left(\frac{d\Gamma}{dy} \right)_{R+L} \xrightarrow{y \rightarrow 0} \Gamma_0 \frac{\alpha}{6\pi} \frac{1}{y} [(-17 + 64\lambda^2 - 64\lambda^6 + 17\lambda^8) + (-12 + 144\lambda^4 - 12\lambda^8) \log(\lambda)]. \tag{15}$$

In the limit of small λ , this reduces to the approximate form

$$\left(\frac{d\Gamma}{dy}\right)_{\text{R+L}} \xrightarrow{\lambda \rightarrow 0} \Gamma_0 \frac{\alpha}{6\pi} \frac{1}{y} [-17 - 12 \log(\lambda)], \quad (16)$$

which agrees with the old calculation of Eckstein and Pratt [11] and Kinoshita and Sirlin [12], in which terms of order λ^2 and higher powers were neglected. The integrated rate for $y > y_0$ is

$$\Gamma_{\text{R+L}}(y_0; \lambda) \xrightarrow{\lambda \rightarrow 0, y_0 \rightarrow 0} \Gamma_0 \frac{\alpha}{\pi} \left[\log(\lambda) \left(2 \log(y_0) + \frac{7}{3} \right) + \frac{17}{6} \log(y_0) - \frac{\pi^2}{3} + \frac{13409}{2520} \right], \quad (17)$$

which agrees with Ref. [11], except in the constant (non-logarithmic) term, which was $-\pi^2/6 + 601/144$ in the old calculation.

3.3 Electron energy spectrum

The exact result for the electron energy spectrum $(d\Gamma/dx)_{\text{R+L}}$ is given in Eq.(A.3) of the Appendix.

The normalized electron energy spectrum is shown in Fig.(2a). In the limit $\lambda \rightarrow 0$ we have for the

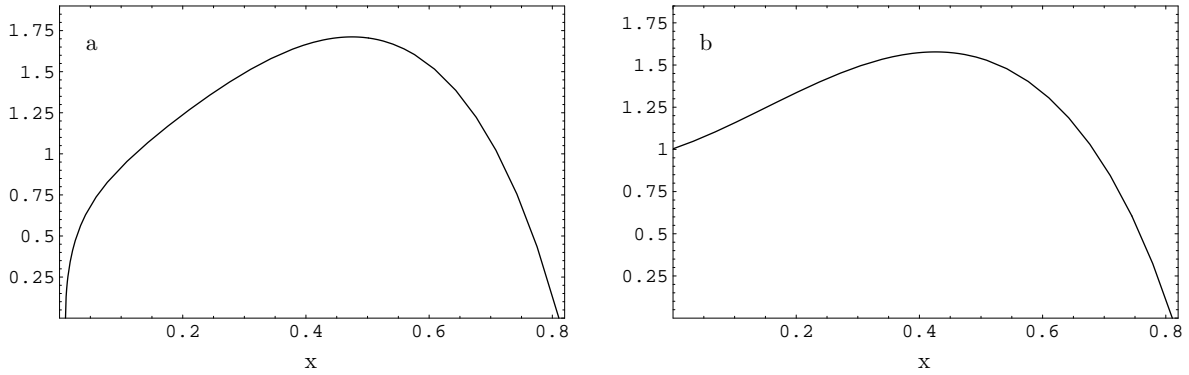


Figure 2: Normalized electron energy spectrum $(\Gamma_{\text{R+L}})^{-1} \left(\frac{d\Gamma}{dx}\right)_{\text{R+L}}$ for $y_0 \approx 0.189$ ($E_{\gamma 0} = 10$ MeV) and a) $\lambda = m_e/m_\mu \approx 1/207$, b) $\lambda \rightarrow 0$.

x -spectrum

$$\begin{aligned} \lim_{\lambda \rightarrow 0} (\Gamma_{\text{R+L}})^{-1} \left(\frac{d\Gamma}{dx}\right)_{\text{R+L}} &= \left\{ (1 - y_0 - x) [-5 - 5 y_0 + 4 y_0^2 + x (-17 + 14 y_0) + 34 x^2] \right. \\ &\quad \left. + 12 x^2 (-3 + 2 x) \log\left(\frac{1-x}{y_0}\right) \right\} \\ &\quad \times \left[(1 - y_0) (7 - 3 y_0 + 3 y_0^2 - y_0^3) + 6 \log(y_0) \right]^{-1}. \end{aligned} \quad (18)$$

This is shown in Fig.(2b).

In the limit $y_0 \rightarrow 0$ we reproduce the spectrum for non-radiative muon decay

$$\lim_{\lambda \rightarrow 0, y_0 \rightarrow 0} (\Gamma_{\text{R+L}})^{-1} \left(\frac{d\Gamma}{dx}\right)_{\text{R+L}} = (\Gamma_{\text{R+L}})^{-1} \left(\frac{d\Gamma}{dx}\right)^{\text{non-rad}} = 2 x^2 (3 - 2 x). \quad (19)$$

4 Spectra for Right- and Left-handed Electrons

The spectra when the final electron is polarized in the state R or L are obtained using Eq.(8). We will emphasize the case R, which is the one which behaves in an unexpected way in the $\lambda \rightarrow 0$ limit [1, 9]. The corresponding spectra for the state L are obtained by subtraction from the unpolarized result L+R discussed in Sec.3.

4.1 Dalitz plot for R-Electrons

$$\begin{aligned}
\left(\frac{d\Gamma}{dx dy}\right)_R &= \Gamma_0 \frac{\alpha}{12\pi} \frac{1}{\mathcal{A}} \frac{1}{y} \{36 \mathcal{A}^2 y^2 + \mathcal{A}(36 y^2 - 60 x y^2 - 24 y^3) + 12 \mathcal{A} \lambda^4 (-8 + y^2) \\
&\quad + \lambda^2 [-288 \mathcal{A} + 96 \mathcal{A}^2 + 192 \mathcal{A} x - 72 \mathcal{A}^2 x + 24 \mathcal{A} x^2 + 192 \mathcal{A} y \\
&\quad \quad - 72 \mathcal{A}^2 y + 72 \mathcal{A} x y - 18 \mathcal{A}^2 x y + 6 \mathcal{A} x^2 y + 48 \mathcal{A} y^2 + 4 \mathcal{A}^2 y^2 \\
&\quad \quad - 52 \mathcal{A} x y^2 + 9 \mathcal{A}^2 x y^2 - 3 \mathcal{A} x^2 y^2 - 24 \mathcal{A} y^3 - 4 \mathcal{A}^2 y^3 + 16 \mathcal{A} x y^3] \\
&\quad + \mathcal{A}(\mathcal{A} - x) [-72 x + 48 x^2 - 72 y + 78 x y + 24 x^2 y + 33 x y^2 \\
&\quad \quad - 10 x^2 y^2 + 12 y^3 - 6 x y^3 + 4 x^2 y^3] \\
&\quad + \mathcal{L} [-12(\mathcal{A} - x)(-3 + 2x + 2y)(2x^2 + 2xy + y^2) \\
&\quad \quad + \lambda^4(96x - 192y + 72\mathcal{A}y - 24xy + 48y^2) \\
&\quad \quad + \lambda^2(288x - 96\mathcal{A}x - 192x^2 + 72\mathcal{A}x^2 - 24x^3 + 72\mathcal{A}y - 264xy \\
&\quad \quad \quad - 24\mathcal{A}xy + 72x^2y - 48y^2 - 60\mathcal{A}y^2 + 84xy^2 + 48y^3)] \}. \tag{20}
\end{aligned}$$

In the limit $\lambda \rightarrow 0$ we obtain

$$\lim_{\lambda \rightarrow 0} \left(\frac{d\Gamma}{dx dy}\right)_R = \Gamma_0 \frac{\alpha}{\pi} y(3 - 2x - 2y). \tag{21}$$

This limiting result coincides with what one obtains on the basis of the helicity-flip splitting function. Denoting the electron spectrum in the non-radiative decay $(d\Gamma/dx_0)^{\text{non-rad}}$, the spectrum after helicity-flip bremsstrahlung is

$$\left(\frac{d\Gamma}{dx_0 dz}\right)_R = \left(\frac{d\Gamma}{dx_0}\right)^{\text{non-rad}} D_{\text{hf}}(z). \tag{22}$$

Noting that $y = x_0 z$, $x = x_0(1 - z)$, and recalling that

$$\left(\frac{d\Gamma}{dx_0}\right)^{\text{non-rad}} = \Gamma_0 2x_0^2(3 - 2x_0), \quad D_{\text{hf}}(z) = \frac{\alpha}{2\pi} z, \tag{23}$$

we obtain

$$\left(\frac{d\Gamma}{dx dy}\right)_R = \frac{1}{x_0} \left(\frac{d\Gamma}{dx_0 dz}\right)_R = \Gamma_0 \frac{\alpha}{\pi} y(3 - 2x - 2y), \tag{24}$$

exactly as in Eq.(21).

4.2 Photon-Spectra for R- and L-electrons

Of particular interest is the photon energy spectrum associated with the right-handed polarization state of the electron, which is naively forbidden in the $\lambda \rightarrow 0$ limit. The corresponding spectrum for L-electrons may be obtained by subtraction from Eq.(A.1). The exact result for $(d\Gamma/dy)_R$ is stated in Eq.(A.5). In the limit $m_e/m_\mu \rightarrow 0$ one obtains

$$\lim_{\lambda \rightarrow 0} \left(\frac{d\Gamma}{dy}\right)_R = \Gamma_0 \frac{\alpha}{\pi} y(1 - y)(2 - y), \tag{25}$$

which is the result derived in [1] on the basis of the helicity-flip fragmentation function $D_{\text{hf}}(z)$. The spectrum for $\lambda \neq 0$ is plotted in Fig.(3). The striking feature is the appearance of a divergence at $y = 0$. This is connected with the fact that for $m_e \neq 0$, helicity is not a good quantum number. As a consequence, ordinary (non-flip) bremsstrahlung, diverging as $1/y$ at small y , is partly transmitted to the final state with electron polarization $s_e = s_e^R$. This contribution vanishes in the limit $\lambda \rightarrow 0$, leaving behind the anomalous (helicity-flip) contribution in Eq.(25). This anomalous bremsstrahlung integrates to a decay width

$$\Gamma_R = \Gamma_0 \frac{\alpha}{4\pi} (1 - y_0)(1 + y_0 - 3y_0^2 + y_0^3), \tag{26}$$

which is the contribution of right-handed electrons to the muon decay width in the $\lambda \rightarrow 0$ limit [1]. The exact expression for $\Gamma_R(y_0)$ and the corresponding left-handed rate $\Gamma_L(y_0)$ are plotted in Fig.(4). From these, we obtain the longitudinal polarization

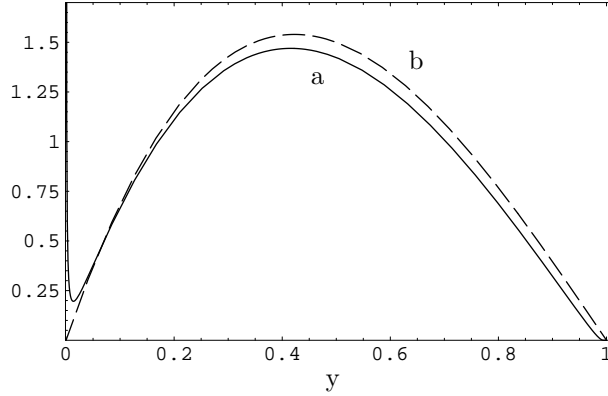


Figure 3: Photon energy spectrum $\left(\frac{d\Gamma}{dy}\right)_R$ for right-handed electrons in units of $\Gamma_0 \frac{\alpha}{4\pi}$ for a) $\lambda = 1/207$, b) $\lambda \rightarrow 0$.

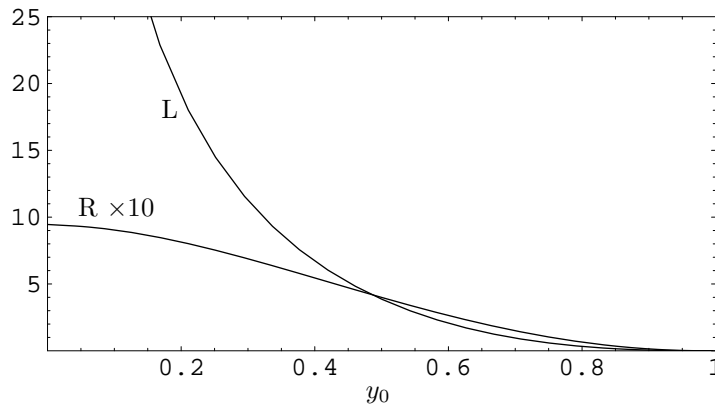


Figure 4: Integrated rates for R- and L-electrons $\Gamma_{R,L}(y_0)$ in units of $\Gamma_0 \frac{\alpha}{4\pi}$ as function of minimum photon energy y_0 .

$$P_L(y_0) := \frac{\Gamma_R(y_0) - \Gamma_L(y_0)}{\Gamma_R(y_0) + \Gamma_L(y_0)} \quad (27)$$

plotted in Fig.(5). This figure demonstrates the presence of a significant right-handed electron component in radiative muon decay, which becomes as probable as the left-handed component at high photon energies. To illustrate the approach to the chiral limit $\lambda \rightarrow 0$, we have also shown in Fig.(5) the polarization of the electron in the decay $\tau^- \rightarrow e^- \bar{\nu}_e \nu_\tau \gamma$. In the chiral limit $\lambda \rightarrow 0$ the longitudinal polarization goes from $P_L = -1$ to $P_L = 0$ like a step-function at $y_0 = 1$.

4.3 Electron Energy Spectra for R- and L-electrons

The formula for the electron energy spectrum $(d\Gamma/dx)_R$ for right-handed electrons is given in Eq.(A.7), and may be compared with the unpolarized spectrum $(d\Gamma/dx)_{R+L}$ in Eq.(A.3) We have verified that in the limit $\lambda \rightarrow 0$, the right-handed spectrum takes the form

$$\left(\frac{d\Gamma}{dx}\right)_R \xrightarrow{\lambda \rightarrow 0} \Gamma_0 \frac{\alpha}{6\pi} (1 - y_0 - x) [5 + 5y_0 - 4y_0^2 + x(-7 - 2y_0) + 2x^2]. \quad (28)$$

This is exactly the result derived in Ref.[1] on the basis of the fragmentation function $D_{\text{hf}}(z)$.

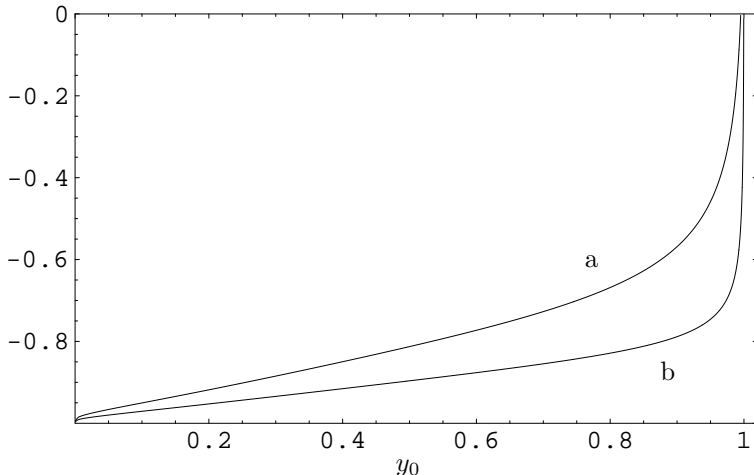


Figure 5: Longitudinal polarization of electron P_L as function of minimum photon energy y_0 : a) $\mu \rightarrow e$ decay, b) $\tau \rightarrow e$ decay.

5 Discussion of the Collinear Region

A question of interest is the behaviour of helicity-flip and helicity-non-flip bremsstrahlung in the collinear region, $\theta \approx 0$, where θ is the angle between the photon and electron in the final state. To this end, we have calculated exactly the distribution $(d\Gamma/d\cos(\theta))_{R,L}$. The analytic results are, however, too lengthy to be written down here. The left- and right-handed spectra for $\lambda = 1/207$, in the small angle region, are plotted in Fig.(6). The longitudinal polarization of the electron as a function of θ is shown in Fig.(7), and, changes

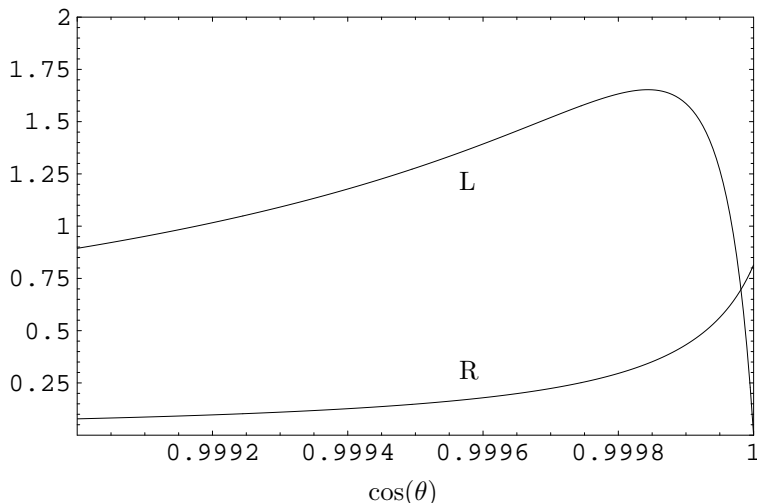


Figure 6: $\cos(\theta)$ spectrum $(\frac{d\Gamma}{d\cos(\theta)})_{L,R}$ for $\lambda = 1/207$ and $y_0 = 0.189$ in units of Γ_0 .

from the V-A value $P_L \approx -1$ to the value $P_L \approx +1$ in the forward direction. From the exact expressions we have derived the behaviour in the chiral limit $\lambda \rightarrow 0$. For $\theta \neq 0$ and $\lambda \rightarrow 0$, we find

$$\begin{aligned} \left(\frac{d\Gamma}{d\cos(\theta)}\right)_R &\xrightarrow{\lambda \rightarrow 0} \Gamma_0 \frac{\alpha}{6\pi} \pi \lambda \frac{1}{\theta^3} (1 - y_0) (5 + 5y_0 - 4y_0^2), \\ \left(\frac{d\Gamma}{d\cos(\theta)}\right)_L &\xrightarrow{\lambda \rightarrow 0} \Gamma_0 \frac{\alpha}{3\pi} \frac{1}{\theta^2} [-7 + 10y_0 - 6y_0^2 + 4y_0^3 - y_0^4 - 6\log(y_0)]. \end{aligned} \quad (29)$$

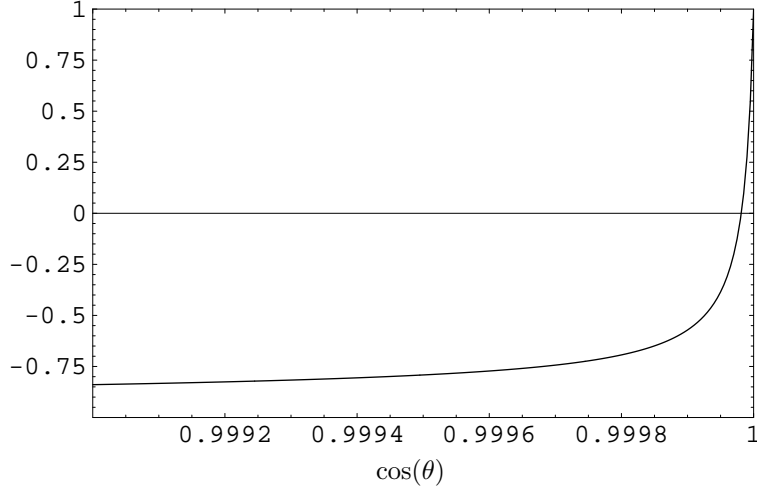


Figure 7: Longitudinal polarization P_L for $\lambda = 1/207$ and $y_0 = 0.189$.

Note that, in the chiral limit, the λ/θ^3 behaviour of $(d\Gamma/d\cos(\theta))_R$ refers to the opening angle of the electron and photon in the final state. The corresponding λ^2/θ^4 behaviour of the helicity-flip scattering cross section (Eq.(1)) refers to the angle between the photon and the incident electron.

We have also derived the value of $(d\Gamma/d\cos(\theta))$ in the forward direction ($\theta = 0$), for small λ :

$$\begin{aligned} \left(\frac{d\Gamma}{d\cos(\theta)}\right)_R \Big|_{\theta=0} &= \Gamma_0 \frac{\alpha}{\pi} \frac{1}{360} \frac{1}{\lambda^2} (1-y_0)^4 (4 + 16y_0 - 5y_0^2) \\ \left(\frac{d\Gamma}{d\cos(\theta)}\right)_L \Big|_{\theta=0} &= \Gamma_0 \frac{\alpha}{\pi} \frac{1}{120} (1-y_0)^4 (1 + 4y_0). \end{aligned} \quad (30)$$

We have found that the angular distribution $(d\Gamma/d\cos(\theta))_R$ connected with helicity-flip bremsstrahlung can be simulated by the following ansatz for the differential decay spectrum (where the label ‘‘APP’’ connotes ‘‘approximate’’):

$$\left(\frac{d\Gamma}{dx dy d\cos(\theta)}\right)_R^{\text{APP}} = \Gamma_0 \frac{2\alpha}{\pi} \lambda^2 y (3 - 2x - 2y) \frac{1}{(x - \cos(\theta) \mathcal{A})^2}. \quad (31)$$

When integrated over $\cos(\theta)$, this spectrum, in the limit $\lambda \rightarrow 0$, yields the Dalitz pair distribution given in Eq.(21). After integration over x and y we obtain an angular distribution $(d\Gamma/d\cos(\theta))_R^{\text{APP}}$ which agrees with the exact calculation over a wide range of angles. This formula is particularly simple for $y_0 = 0$:

$$\left(\frac{d\Gamma(y_0 = 0)}{d\cos(\theta)}\right)_R^{\text{APP}} \xrightarrow{\lambda \rightarrow 0} \Gamma_0 \frac{\alpha}{\pi} \frac{5}{6} \lambda \left[1 + (\pi - \theta) \frac{\cos(\theta)}{\sin(\theta)}\right] \frac{1}{\sin^2(\theta)}, \quad (32)$$

which agrees with the small angle result given in Eq.(29). Similarly, in the forward direction ($\theta = 0$), for small values of λ , the approximate representation Eq.(31) reproduces the result given in Eq.(30).

6 Conclusions

The purpose of this paper was to examine the dependence of the radiative decay $\mu^- \rightarrow e^- \bar{\nu}_e \nu_\mu \gamma$ on the helicity of the final electron, in order to demonstrate the presence of right-handed electrons, even in the chiral limit $m_e \rightarrow 0$. This non-intuitive feature is a consequence of helicity-flip bremsstrahlung in QED, and was discussed in [1] with the help of the helicity-flip splitting function derived in [2]. We have now calculated the complete helicity-dependent spectrum of this decay from first principles, without neglecting the electron mass, and have shown that the results of [1] are reproduced in the limit $\lambda \rightarrow 0$. The presence

of right-handed electrons manifests itself in the longitudinal polarization $P_L = (\Gamma_R - \Gamma_L)/(\Gamma_R + \Gamma_L)$ which deviates from the naive V-A value $P_L = -1$ even in the limit $\lambda \rightarrow 0$. The dependence of the polarization on the photon energy cut y_0 , Fig.(5), shows that right-handed electrons occur predominantly with high energy photons. A characteristic signature of wrong-helicity electrons is also present in the opening-angle distribution $d\Gamma/d\cos(\theta)$, where the collinear region $\theta \lesssim \lambda/(1 - y_0)$ is dominated by right-handed electrons. The fact that helicity-flip bremsstrahlung in the chiral limit $m_e \rightarrow 0$ can be exactly reproduced by the simple and universal splitting function $D_{\text{hf}}(z)$ in many different processes, is suggestive of a relationship to the chiral anomaly in QED [13, 14, 15].

Appendix A

$$\begin{aligned}
\left(\frac{d\Gamma}{dy}\right)_{\text{R+L}} &= \int_{2\lambda}^{x_m(y)} dx \left(\frac{d\Gamma}{dx dy}\right)_{\text{R+L}} \\
&= \Gamma_0 \frac{\alpha}{36\pi} \frac{1}{y} \left\{ [(-102 + 46y - 95y^2 + 109y^3 - 45y^4 + 21y^5 - 6y^6)(1-y) \right. \\
&\quad + 6\lambda^2(64 - 250y + 386y^2 - 240y^3 + 67y^4 - 20y^5 + 5y^6)(1-y)^{-1} \\
&\quad + 18\lambda^4 y(18 + 12y - 40y^2 + 11y^3 + 3y^4)(1-y)^{-2} \\
&\quad + 2\lambda^6(-192 + 622y - 856y^2 + 552y^3 - 105y^4 - 21y^5)(1-y)^{-4} \\
&\quad + 3\lambda^8(34 - 64y - 13y^2 + 4y^3)(1-y)^{-4}] \\
&\quad + [24(-3 + 2y - 4y^2 + 2y^3)(1-y) + 72\lambda^2 y(-13 + 19y - 7y^2)(1-y)^{-1} \\
&\quad + 72\lambda^4(12 - 27y + 18y^2 - 5y^3)(1-y)^{-1} + 24\lambda^6 y(5 + 15y - 18y^2)(1-y)^{-3} \\
&\quad \left. + 72\lambda^8(-1 + 2y)(1-y)^{-4}] \log\left(\frac{\lambda}{1-y}\right) \right\}. \tag{A.1}
\end{aligned}$$

$$\left(\frac{d\Gamma}{dx}\right)_{\text{R+L}} = \Gamma_0 \frac{\alpha}{\pi} \frac{1}{\mathcal{A}} u^{-4} (u^2 - \lambda^2) \left[k_1 + \log\left(\frac{u}{\lambda}\right) k_2 + \log\left(\frac{1-u}{y_0}\right) k_3 + \log\left(\frac{u}{\lambda}\right) \log\left(\frac{1-u}{y_0}\right) k_4 \right], \tag{A.2}$$

where $u = (x + \mathcal{A})/2$, and

$$\begin{aligned}
k_1 &:= \frac{1}{36} (u^2 - \lambda^2) (1 - y_0 - u) \left[u^2 (-300 + 399u + 71u^2 + 2u^3 + 8u^4 + 132y_0 + 63uy_0 - 10u^2y_0 \right. \\
&\quad \left. - 8u^3y_0 + 24y_0^2 - 12uy_0^2 + 8u^2y_0^2) \right. \\
&\quad \left. + \lambda^2 u (555 - 259u - 61u^2 - 19u^3 + 87y_0 - 28uy_0 + 19u^2y_0 \right. \\
&\quad \left. - 12y_0^2 + 8uy_0^2) \right. \\
&\quad \left. + \lambda^4 (122 - 67u - 19u^2 - 22y_0 + 19uy_0 + 8y_0^2) \right], \\
k_2 &:= \frac{1}{3} u (1 - y_0 - u) \left[u^2 (5 + 17u - 34u^2 + 5y_0 - 14uy_0 - 4y_0^2) + 3\lambda^2 u (6 - 19u + u^2 - 6y_0 - 5uy_0) \right. \\
&\quad \left. + 12\lambda^4 (-4 - u + 3u^2) \right], \\
k_3 &:= 4(\lambda^2 - u^2) [u^3(3 - 2u) + \lambda^2 u(3 - 8u + 3u^2) + \lambda^4(-2 + 3u)], \\
k_4 &:= 4(\lambda^2 + u^2) [u^3(3 - 2u) + \lambda^2 u(3 - 8u + 3u^2) + \lambda^4(-2 + 3u)], \tag{A.3}
\end{aligned}$$

$$\begin{aligned} \left(\frac{d\Gamma}{dy}\right)_R &= \int_{2\lambda}^{x_m(y)} dx \left(\frac{d\Gamma}{dx dy}\right)_R \\ &= \Gamma_0 \frac{\alpha}{\pi} \left[y(1-y)(2-y) + h_1 + \log\left(\frac{1-y}{\lambda}\right) h_2 + \log^2\left(\frac{1-y}{\lambda}\right) h_3 \right], \end{aligned} \quad (\text{A.4})$$

where

$$\begin{aligned} h_1 &:= 4\lambda y(-3+2y) + \frac{1}{18}\lambda^2 \frac{1}{y} \frac{1}{1-y} (-248 + 176y + 489y^2 - 304y^3 - 53y^4 - 6y^5) \\ &\quad + \frac{8}{9}\lambda^3 \frac{1}{y} (48 - 10y + 15y^2 + 3y^3) + \frac{1}{4}\lambda^4 \frac{1}{y} \frac{1}{(1-y)^2} (-150 + 320y - 209y^2 + 16y^3 + 29y^4 - 2y^5) \\ &\quad + \frac{4}{9}\lambda^5 \frac{1}{y} (32 - 12y - 3y^2) + \frac{1}{18}\lambda^6 \frac{1}{y} \frac{1}{(1-y)^3} (-120 + 412y - 465y^2 + 114y^3 + 18y^4) \\ &\quad + \frac{1}{36}\lambda^8 \frac{1}{y} \frac{1}{(1-y)^4} (38 - 140y - 21y^2 + 6y^3), \\ h_2 &:= \frac{2}{3}\lambda^2 \frac{1}{y} \frac{1}{1-y} (8 + 13y - 30y^2 + 7y^3 + 5y^4) + \lambda^4 \frac{1}{y} \frac{1}{1-y} (-16 + 22y - 19y^2 + 3y^3) \\ &\quad + \frac{4}{3}\lambda^6 \frac{1}{(1-y)^3} (-1 - 6y + 6y^2) + \frac{2}{3}\lambda^8 \frac{1}{y} \frac{1}{(1-y)^4} (1 - 4y), \\ h_3 &:= 2\lambda^2(1-y)(-3-y) + 2\lambda^4 \frac{1}{y} (-2 - y + y^2). \end{aligned} \quad (\text{A.5})$$

$$\left(\frac{d\Gamma}{dx}\right)_R = \Gamma_0 \frac{\alpha}{\pi} \left[j_1 + \log\left(\frac{u}{\lambda}\right) j_2 + \log\left(\frac{1-u}{y_0}\right) j_3 + \log\left(\frac{u}{\lambda}\right) \log\left(\frac{1-u}{y_0}\right) j_4 \right], \quad (\text{A.6})$$

where

$$\begin{aligned} j_1 &:= \frac{1}{36} \frac{1}{u^3} (1 - y_0 - u) \left\{ u^3 [30 + 12u^2 + u(-42 - 12y_0) + 30y_0 - 24y_0^2] \right. \\ &\quad + \lambda^2 u^2 [264 - 168y_0 - 24y_0^2 + u(261 - 15y_0 - 12y_0^2) \\ &\quad + u^2(-155 - 26y_0 + 4y_0^2) + u^3(-5 + 5y_0) + u^4(-5)] \\ &\quad + \lambda^4 u [-555 - 87y_0 + 12y_0^2 + u(199 - 32y_0 + 4y_0^2) \\ &\quad + u^2(73 + 5y_0) + u^3(-5)] \\ &\quad \left. + \lambda^6 [-122 + 22y_0 - 8y_0^2 + 10u(4 - y_0) + 10u^2] \right\}, \\ j_2 &:= \frac{1}{3} \frac{1}{u^2} \frac{\lambda^2}{u^2 - \lambda^2} \left\{ u^2(1 - y_0 - u) [-5 - 5y_0 + 4y_0^2 + u(-19 + 12y_0 + 4y_0^2) + u^2(-13 - y_0) + 13u^3] \right. \\ &\quad + 6\lambda^2 u(1 - y_0 - u) [-3 + 3y_0 + u(2 + 3y_0) + u^2(-4 + y_0) + u^3] \\ &\quad \left. + 24\lambda^4(2 - u)(1 + u)(1 - y_0 - u) \right\}, \\ j_3 &:= 4 \frac{1}{u^3} \lambda^2 (1 - u) (\lambda^2 - u^2) (-2\lambda^2 + 3u - u^2), \\ j_4 &:= 4 \frac{1}{u^3} \lambda^2 (1 - u) (\lambda^2 + u^2) (-2\lambda^2 + 3u - u^2). \end{aligned} \quad (\text{A.7})$$

References

- [1] L. M. Sehgal, Phys. Lett. B **569**, 25 (2003).
- [2] B. Falk and L. M. Sehgal, Phys. Lett. B **325**, 509 (1994).
- [3] H. F. Contopanagos and M. B. Einhorn, Nucl. Phys. B **377**, 20 (1992).
- [4] S. Jadach, J. H. Kühn, R. G. Stuart and Z. Was, Z. Phys. C **38**, 609 (1988) [Erratum-ibid. C **45**, 528 (1990)].
- [5] L. Trentadue and M. Verbeni, Phys. Lett. B **478**, 137 (2000) and Nucl. Phys. B **583**, 307 (2000); A. V. Smilga, Comments Nucl. Part. Phys. **20**, 69 (1991).
- [6] S. Groote, J. G. Körner and M. M. Tung, Z. Phys. C **70**, 281 (1996).
- [7] W. E. Fischer and F. Scheck, Nucl. Phys. B **83**, 25 (1974).
- [8] T. D. Lee and M. Nauenberg, Phys. Rev. **133**, B1549 (1964).
- [9] M. Fischer, S. Groote, J. G. Körner and M. C. Mauser, Phys. Rev. D **67**, 113008 (2003).
- [10] A. Fischer, T. Kurosu and F. Savatier, Phys. Rev. D **49**, 3426 (1994).
- [11] S. G. Eckstein and R. R. Pratt, Ann. Phys. **8**, 297 (1959).
- [12] T. Kinoshita and A. Sirlin, Phys. Rev. **113**, 1652 (1959).
- [13] A. D. Dolgov and V. I. Zakharov, Nucl. Phys. B **27**, 525 (1971); K. Huang, *Quarks, Leptons And Gauge Fields* (World Scientific, Singapore, 1992); J. Horejsi, Czech. J. Phys. **42**, 241 (1992).
- [14] A. Freund and L. M. Sehgal, Phys. Lett. B **341**, 90 (1994).
- [15] R. D. Carlitz, J. C. Collins and A. H. Mueller, Phys. Lett. B **214**, 229 (1988).